This manuscript was accepted and published in Applied Spectroscopy

http://journals.sagepub.com/doi/10.1177/0003702817752112

The thermal boundary layer effects on line-of-sight TDLAS gas concentration measurements

Zhechao Qu, Olav Werhahn, Volker Ebert

Physikalisch-Technische Bundesanstalt, Bundesallee 100, D-38116 Braunschweig, Germany

Email: volker.ebert@ptb.de

Abstract

The effects of thermal boundary layers on TDLAS measurement results must be quantified when using the line-of-sight (LOS) tunable diode laser absorption spectroscopy (TDLAS) under heterogeneous conditions. In this paper, a new methodology based on spectral simulation is presented quantifying the LOS TDLAS measurement deviation under heterogenous conditions with thermal boundary layers. The effects of different temperature gradients and thermal boundary layer thickness on spectral collisional widths and gas concentration measurements are quantified. A CO_2 TDLAS spectrometer, which has two gas cells to generate the temperature heterogeneity, was employed to validate the simulation results. The measured deviations and collisional widths are in very good agreement with the simulated results for different temperature heterogenous conditions. We demonstrate quantification of thermal boundary layers' thickness with proposed method by extracting the collisional width from the path-integrated spectrum.

Key words

TDLAS, boundary layer, temperature heterogeneity, gas concentration, line-of-sight

Introduction

Tunable diode laser absorption spectroscopy (TDLAS) is frequently used in science and industry for online and in situ gas analysis and has become a proven method of gas diagnostics.[1-5] Online in situ open-path TDLAS instruments do not require to take a gas sample into a closed measurement cell. This has the advantage of circumventing typical sampling problems like chemical reactions in the sampling line, delay and integration effects due to the gas transport, or wall adsorption in the sampling pipes. Absolute chemical species measurements using calibration-free TDLAS techniques need accurate measurements of the physicochemical boundary layers' conditions,[1] e.g. parameters like gas temperature and pressure. This TDLAS

in nature is one of the line-of-sight (LOS) absorption spectroscopy techniques, and its application is normally limited to flow fields with homogenous conditions, or negligible heterogeneities. In most single wavelength LOS TDLAS applications, homogeneous conditions are assumed. This constitutes a drawback in many applications, for example, when large and unexpected temperature and/or concentration gradients along the LOS may occur. The effect of boundary layers on experimental data must be well understood for a successful diagnostic measurement using LOS absorption spectroscopy.[6-9]

A lot of research efforts have been invested in absorption spectroscopy strategies for minimizing the effects of boundary layers on the LOS TDLAS measurements[6, 10-19] or recovering spatial distribution by using tomographic inversion techniques.[20-24] In combustion environments, less temperature dependence lines were used under temperature heterogenous and temperature varying conditions to minimize the boundary layers effects on gas concentration measurements,[11-12] both transitions and modulation depths were carefully selected to minimize the variation and heterogeneities in pressure and absorber concentration to archive an accurate gas temperature measurement in the gasifier reactor core based on two-line thermometry.[14] A strategy of wavelength-modulation spectroscopy (WMS) based TDLAS was developed immune to the errors of two-line thermometry temperature measurements caused by the LOS heterogeneities in temperature, pressure, and concentration by using two absorption transitions with strengths that scale linearly with temperature over the domain of the temperature heterogeneity.[16] The error caused by temperature and velocity heterogeneities along the LOS in velocity measurement using WMS-TDLAS was analysed.[17-18] There has been a lack of quantitative analysis the effect of temperature heterogeneity on the LOS laser spectroscopy for gas concentration measurements.

An alternative and more complicated strategy that can significantly improve on the LOS TDLAS under heterogeneous conditions is the combination of tomographic absorption spectroscopy (TAS).[20] The TAS solution for spatially resolved heterogeneous fields from the LOS data, multiple measurement paths[24]/wavelengths[21-23] have to be combined into a tomographic setup, the heterogeneous temperature or concentration distributions can be retrieved by making the use of nonlinear and linear regularization methods. It is obvious that the TAS makes both instrument and data analysis more complicated and costly than the single wavelength TDLAS.

In heterogeneous conditions, the path integrated spectrum of direct TDLAS (dTDLAS) is different than the simulation performed with path averaged condition along the LOS. The errors of concentration measurements can be deduced by comparing the integrated absorption coefficient[6] or the peak absorbance[16] from the path integrated spectrum and that of the simulation performed with the path averaged homogenous condition. But the path-averaged information, e.g. temperature, is not always available in many applications such as cross stack emission monitoring. Using the optical transfer standards-dTDLAS under heterogeneous conditions,[25-26] the path-integrated spectra are measured together with temperature and pressure measurements (one or several sampling points along the LOS). The question is how to evaluate the measured spectra. The derived concentration is different when using path-averaged, wall or core temperature/pressure to evaluate the spectra. It is essential to know the deviation of the deduced concentration from the measured path integrated spectrum when heterogeneity presents.

In this work, we present a methodology for quantifying the deviation of dTDLAS concentration measurements under the conditions with thermal boundary layers. The use of two-cell based dTDLAS CO_2 spectrometer enabled validation of the simulated results. It was shown that the simulated results had very good agreement with the measurements. The method was also applied to estimation of thermal boundary layer's thickness from the collisional widths of path-integrated spectra and to investigate temperature heterogeneous effects.

Theory

Tunable diode laser absorption spectroscopy

In TDLAS, the wavelength λ of a tunable laser is rapidly scanned across a narrow region of the optical spectrum covering one or several electronic, vibrational or rotational-vibrational absorption lines. The intensity of the laser light, $I(\lambda)$, focused onto a photodetector after passing the sample with absorbers can be described by the extended Lambert-Beer law according to

$$I(\lambda) = E(t) + I_0(\lambda) \cdot T(t) \cdot \exp[-S(T) \cdot g(\lambda - \lambda_0) \cdot n \cdot L], \tag{1}$$

with the background emission $E(t)$ at time t, initial laser intensity $I_0(\lambda)$, and the broadband transmission losses $T(t)$ which are synchronously derived from the individual raw signals and absorption profiles. The exponential term embraces the absorption line strength $S(T)$ at gas temperature T, the normalised (area=1) line shape function $g(\lambda-\lambda_0)$ (centred at the wavelength λ_0), the absorber number density n and the optical path length L.

By combining Eq. 1 and the ideal gas law, the gas concentration (amount fraction) x is

$$x = \frac{k_B \cdot T}{S(T) \cdot r_{iso} \cdot L \cdot p_{total}} \int \ln\left(\frac{I(\lambda) - E(t)}{I_0(\lambda) \cdot Tr(t)}\right) \frac{d\lambda}{dt} dt = \frac{k_B \cdot T \cdot A_{line}}{S(T) \cdot r_{iso} \cdot L \cdot p_{total}}, \tag{2}$$

where k_B is the Boltzmann constant, p_{total} is the total pressure of the gas sample, r_{iso} is a correction factor for the isotopic composition in the gas sample, and A_{line} is the line area determined by spectral integration of the measured absorption line over the wavenumber axis. $d\lambda/dt$ describes the dynamic wavelength tuning coefficient of the laser, which has to be determined experimentally. This is extracted from the Airy-signal when the laser light is transmitted through an optical etalon.

The Voigt function was used to model the lineshape of the transition, which considers the combined effects of Doppler and collisional broadening on the spectrum. These effects are characterized by the Doppler broadening full width at half maximum (FWHM), $\Delta\nu_D$ (cm^{-1}), and the collisional-broadening FWHM, $\Delta\nu_L$ (cm^{-1}), given by

$$\Delta\nu_D = \nu_0 \sqrt{\frac{8 k_B T \ln 2}{M c^2}}, \tag{3}$$

$$\Delta\nu_L = 2\gamma_{self} \cdot p_{self} \cdot \left(\frac{T_0}{T}\right)^{n_{self}} + 2\sum_f \gamma_f \cdot p_f \left(\frac{T_0}{T}\right)^{n_f}, \tag{4}$$

where M is the molecular mass of the absorbing species, the coefficients γ_{self} and γ_f are the self and foreign (e.g. air or N_2) broadening coefficients, p_{self} and p_f are the partial pressures of the analyte, e.g. CO_2, and the foreign molecules, respectively, n_{self} and n_f are the temperature dependence of the collisional broadening which must be specifically considered when the temperature is far away from the reference temperature T_0=296 K. Typical values for n_{self} and n_f are between 0.4 and 0.9. Normally, Doppler broadening can be calculated directly using Eq. 3 and thus does not have to be fitted, if the gas temperature is measured in the experiment with sufficient accuracy. When the pressure increases to 1 bar or higher, the Doppler width becomes much smaller than collisional width. In this condition, the Doppler width should be fixed and calculated with Eq. 3 while doing the Voigt lineshape fitting.

In thermal homogenous conditions, the calculation temperature T in Eq. 2, should be known to calculate the gas concentration, and the line strength $S(T)$ according to

$$S(T) = S(T_0) \cdot \frac{Q(T_0)}{Q(T)} \cdot \exp\left[-\frac{h \cdot c \cdot E''}{k_B}\left(\frac{1}{T} - \frac{1}{T_0}\right)\right] \cdot \frac{1 - \exp[-h \cdot c \cdot \nu_0/(k_B \cdot T)]}{1 - \exp[-h \cdot c \cdot \nu_0/(k_B \cdot T_0)]}, \tag{5}$$

where Q is partition sum, h is the Planck constant, c is the speed of light in vacuum, E" is the lower state energy of the transition, ν_0 is the spectral transition wavenumber, and $S(T_0)$ is the line strength given for the reference temperature (T_0=296 K).

It is clear that the gas concentration x, as well as $S(T)$, can be calculated using the calculation temperature T which is constant along the LOS in homogeneous conditions. But, it is not the case in heterogeneous conditions with thermal boundary layers. TDLAS measurements are path-integrated, i.e. the temperature at each point along the beam path is incorporated into the detected absorption feature. Using different calculation temperature (e.g. path-averaged, maximum or minimum temperature along the LOS) derives different concentration result. The effects of the thermal heterogeneity in the test gas on the LOS absorption measurements can be addressed by simulating path-integrated spectra. This allows for heterogeneity effects on concentration measurements to be quantified and enables the development of guidelines for desensitizing the LOS measurements to heterogeneous fields e.g. stacks or combustion chambers.

Line temperature dependence

To estimate the relative influence of thermal boundary layers, the temperature dependence of the target transition line has to be analyzed. Figure 1a shows two forms of the temperature dependence of the CO_2 P36e transition line, one is the number density normalized temperature dependence $S(T)$ with the unit of cm^{-1}/molecules·cm^{-2}, the other is $S(T)/T$ with the unit of cm^{-1}/molecules·cm^{-2}·K. The temperature independence positions of these two forms are 454 K and 321 K for $S(T)$ and $S(T)/T$, respectively. According to Eq. 2, if the species concentration x is to be measured, the temperature dependence of $S(T)/T$ should be analyzed, dashed curve in Figure 1a. Otherwise, number density normalized temperature dependence $S(T)$ is used when measuring the number density n. This paper focuses on the concentration measurement, so that the derivative and temperature coefficient of $S(T)/T$ are shown in Figure 1b. Around the $S(T)/T$ maximum near 321 K the temperature dependence is negligible, whereas for the further distant temperatures the influence of the temperature measurement uncertainty increases. The temperature coefficient shows the line strength $S(T)/T$ changes from -0.4 to 0.8 %/K in the full range. This is beneficial to estimate whether a transition line is good enough for certain applications, especially under heterogenous and varying temperature conditions. If the gas temperature varies along the LOS, the gas concentration cannot be predicted accurately from the measured integrated area without knowledge of the temperature distribution along the LOS.

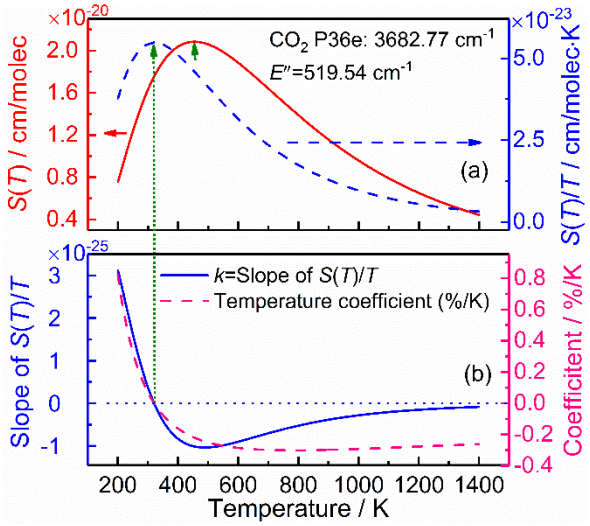

Figure 1. (a) Temperature behavior of the line strength for the CO_2 P36e transition line, the line data are from HITRAN;[27] solid: S(T)--cm/molec; dash: S(T)/T--cm/molec·K. (b) The derivative (solid) and temperature (dash) coefficient of S(T)/T.

Scheme of modelling thermal boundary layer effect

To quantify the deviation of concentration measurements with the LOS TDLAS technique under heterogeneous temperature conditions, we consider a two-zone temperature distribution across the LOS as shown in Figure 2a, with low temperature zone at T_1 and L_1, and T_2 and L_2 for the high temperature zone. To investigate the thermal boundary layer effects, the basic idea is to derive the concentration from a simulated path-integrated spectrum under heterogenous conditions. The different calculation temperature, e.g. path-averaged temperature T_{ave}, maximum temperature along LOS T_{max}, or minimum temperature along LOS T_{min}, used in Eqs. 2 and 5 skews the measurement results differently. The deviation is defined as the discrepancy between the derived concentration and the initial concentration used to simulate the path-integrated spectrum. It is a straightforward way to estimate the deviation of TDALS concentration measurements in real applications. The deviation depends on which calculation temperature is used to evaluate the measured path-integrated spectrum. The simulation routine shown in Fig. 2b was used: A) simulate the path-integrated spectrum under the heterogeneous condition with the input parameters (T_i, L_i, p_i and initial concentration C_i) and the transition line data, e.g. from HITRAN; B) fit the simulated spectrum and derive the area and collisional width; C) choose the calculation temperature (T_{ave}, T_{min} or T_{max}) to derive the concentration x; D) calculate the deviation Δx by comparing the derived concentration x and the value of C_{ave} which is used to simulate the spectrum. This strategy can be applied to the LOS TDLAS to quantify the deviation of concentration measurement under any heterogenous conditions.

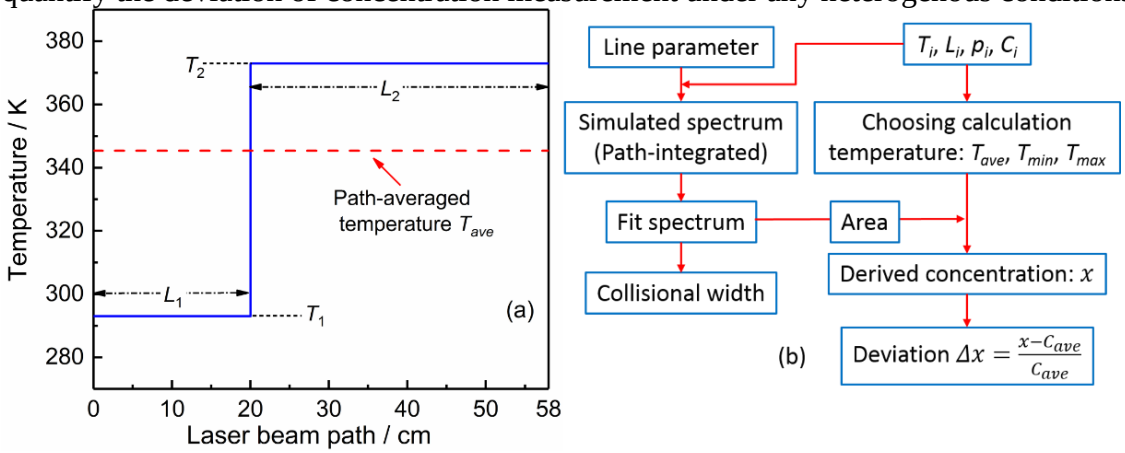

Figure 2. (a) Two-zone temperature distribution across the simulated LOS, low temperature zone with T_1 and L_1, high temperature zone with T_2 and L_2. (b) Flow chart of the simulation scheme to calculate the concentration deviation, T_i, L_i, p_i and C_i are the temperature, path length, pressure and initial concentration of the i-th section, $C_{ave} = \frac{\sum C_i \cdot L_i}{\sum L_i}$(if $C_i \neq C_{i+1}$).

Deviations of concentration measurement under heterogeneous conditions

The strategy of quantifying the deviation of dTDLAS concentration measurements shown in Figure 2b is demonstrated with simulated path-integrated spectra for different thermal boundary layer conditions. More generally, this strategy can be applied to any LOS heterogeneities, not only with heterogeneous temperature distributions, but also heterogeneous concentration profiles. Figure 3 shows the simulated deviations of concentration measurements based on different calculation temperatures (T_{ave}, T_{min} and T_{max}) under two-zone temperature heterogeneities for the CO_2 transition line shown in Fig. 1. In this demonstration, the high T_2 and low T_1 temperatures were fixed at 393 and 293 K, respectively. The high/low temperature path length ratio (L_2/L_1) across the LOS was changed to be representative of different thermal boundary layer thickness. When using the path-averaged temperature T_{ave} as the calculation temperature in Eqs. 2 and 5, the largest deviation appeared at L_2/L_1 around 1 where thermal

boundary layer is largest. Obviously, the deviation increases using calculation temperature of T_{min} (or T_{max}) when the path length ratio L_2/L_1 increases (or decreases). For example, in the scenario of stack monitoring if only wall or core temperature is measured, the maximum deviation of concentration measurement under this two-zone temperature (T_1=293 K, T_2=393 K) distribution is about 4.6 %, this value will change when varying T_1 or T_2 as we can see in the following section. Note that using T_{ave} as calculation temperature doesn't always have lowest deviation which can be seen from Fig. 3. The deviation of derived concentration does not only depend on the LOS temperature profile but also the transition line's temperature dependence $S(T)/T$.

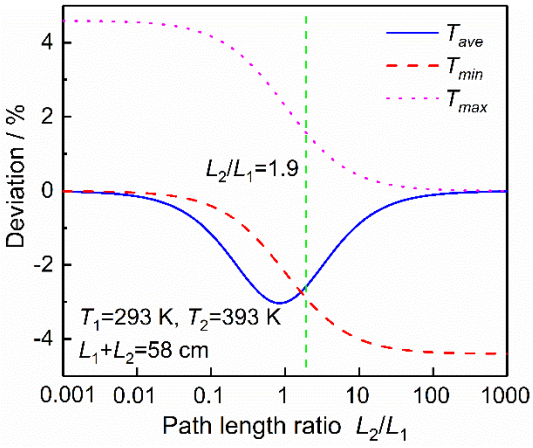

Figure 3. Simulated deviations of concentration measurements based on different calculation temperatures T_{ave}, T_{min}, and T_{max} under two-zone temperature profile as shown in Fig. 2a with different boundary layer thickness.

Figure 4 shows the simulated deviations of a fixed thermal boundary layer thickness L_2/L_1 =1.9 with varying temperatures T_1 and T_2 for P36e CO_2 transition line. Using calculation temperature T_{ave} as shown in Fig. 4a, the deviation (underestimated) increases as T_2 is increasing when T_1 is smaller than 320 K; the deviation (overestimated) increases as T_2 increasing when T_1 larger than 450 K. Figures 4b and 4c show the results using the calculation temperature T_{min} (=T_1) and T_{max} (=T_2), respectively. The derived concentrations under temperature heterogeneities shown in Fig. 4 are always underestimated when using T_{min} as calculation temperature, while overestimated using T_{max}. Different calculation temperature chosen for Eqs. 2 and 5 leads to different deviation. In dTDLAS applications under heterogenous conditions, the transitions line and calculation temperature should be carefully selected to minimize the deviation. In most real scenarios, the real time in situ path-averaged temperature T_{ave} is unavailable for TDLAS spectral evaluation. For example, in stack application, only the wall temperature is measured in most cases, the core temperature is rarely measured. This means only wall temperature (e.g. T_{min}) is available for TDLAS spectrometer to derive the concentration. It is essential to quantify the systematic deviation of implementing the LOS TDLAS under heterogenous conditions with the proposed method in Fig. 2b for an estimated or measured temperature gradient.

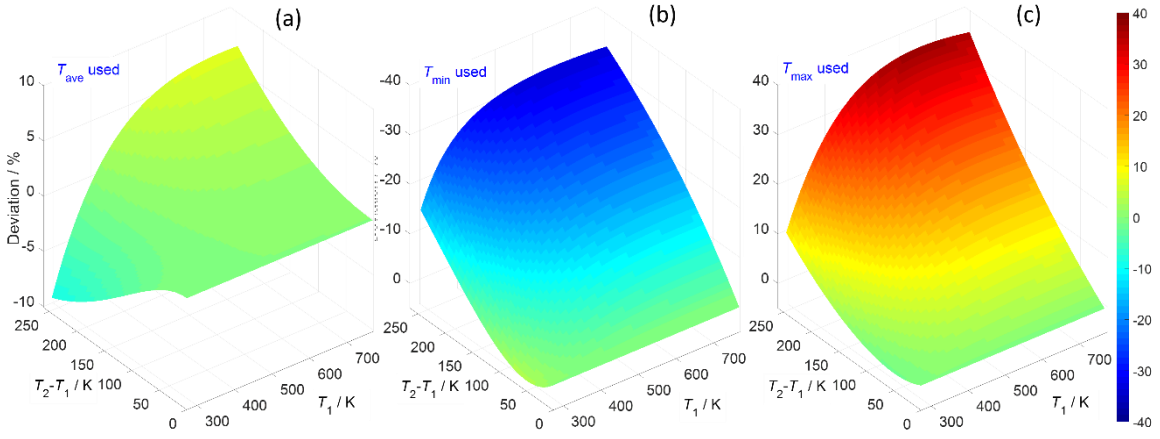

Figure 4. Simulated deviations of concentration measurements with different thermal boundary layers and calculation temperatures. T_{ave} (a), T_{min} (b) and T_{max} (c) was used in Eqs. 2 and 5 to calculate the concentration, respectively.

Thermal boundary layer effects on collisional width

According to Eqs. 3 and 4, the Doppler and collisional widths are nonlinearly dependent on temperature. As a result, when the gas temperature varies along the LOS, both widths from the line shape of path-integrated absorbance spectra are different from homogeneous conditions. Figure 5a shows the collisional widths of the path-integrated spectra under corresponding heterogenous conditions shown in Fig. 3. Note that, the Voigt function was used to fit the path-integrated spectra with fixed Doppler width. Three almost overlapping curves in Fig. 5a are calculated based on different Doppler widths which were calculated based on Eq. 4 using different calculation temperatures (T_{ave}, T_{min} and T_{max}). Because the pressure used in the simulation was 770 mbar, the Doppler width was much smaller than the collisional width, and should be fixed while doing the Voigt fitting. Figure 5b shows the standard deviations of the residuals of Voigt fitting under each condition in Fig. 5a. The largest standard deviation was observed at the condition with the thermal boundary layer ratio L_2/L_1 around 1. The 3D plot in Fig. 5c shows the collisional widths under different temperature heterogeneities. The collisional width monotonically changes with L_2/L_1 for fixed T_1 and T_2. On the other hand, the thermal boundary layer thickness can be roughly estimated by the measured collisional width together with T_1 and T_2. For example, in the applications of the real stack or flat-flame measurements (assuming two-zone temperature profile), based on the wall T_1 and core T_2 temperatures, and measured collisional width of path-integrated spectrum, the thermal boundary layer thickness can be estimated using this simulation method, an example will be shown in section 3. When the boundary layer is very thin (e.g. L_2/L_1<0.1 or L_2/L_1>10), the collisional width weakly decreases with increasing L_2/L_1, there will be a large uncertainty in the thermal boundary layer estimation due to the collisional width is insensitive to the thermal boundary layer when approaching to homogeneous situations.

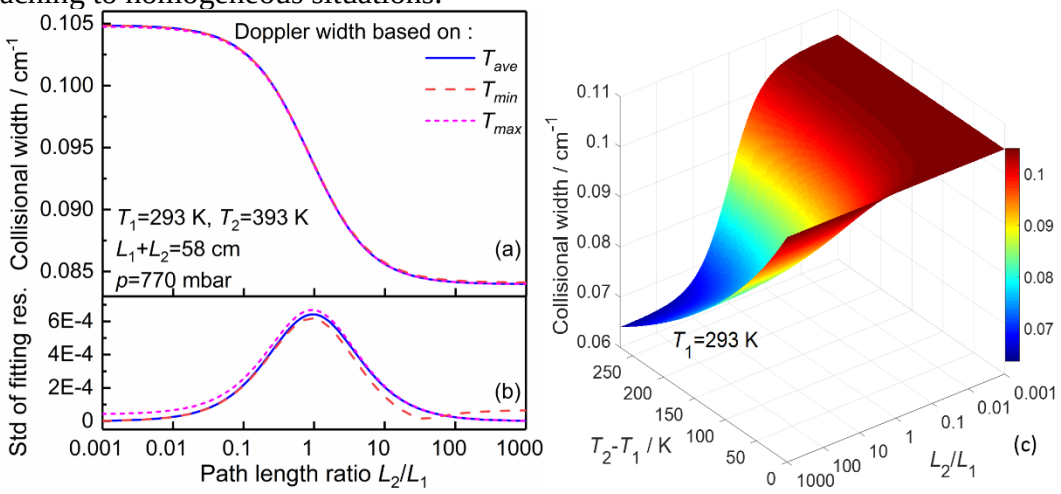

Figure 5. (a) Fitted collisional widths under different boundary layer ratio (L_2/L_1) with L_1+L_2=58 cm, T_1=293 K, T_2=393 K, p=770 mbar, three curves correspond to different Doppler width which was calculated based on different temperature (T_{ave}, T_{min} or T_{max}). (b) Standard deviations of the residuals of Voigt fitting corresponding to the conditions in (a). (c) Fitted collisional widths with varying T_2 (293 to 560 K) and L_2/L_1 (0.001 to 1000).

Validation and demonstration

Spectrometer performance

In the demonstration experiment, a two-zone temperature distribution was created in laboratory setup using two gas cells. A schematic drawing of the experimental setup is shown in Figure 6a. A distributed feedback (DFB) diode laser at 2715 nm (Nanoplus GmbH) which has a tuning rate of 0.4 nm/K by temperature and 0.01 nm/mA by current was used to scan across the CO_2 P36e absorption line.[28] The laser injection current was supplied by a low-noise driver (Thorlabs, LDC8002&TEC8020), which also controlled the diode temperature. The scan was achieved by varying the laser current with a 139.8 Hz triangular wave generated by a function generator (Agilent, 33220A). The laser beam was directed through the gas cells and then focused onto a photodetector. The detector signal was sampled at 600 kHz (National Instruments, PXIe-6124). Data acquisition and spectral fitting were controlled via LabVIEW.

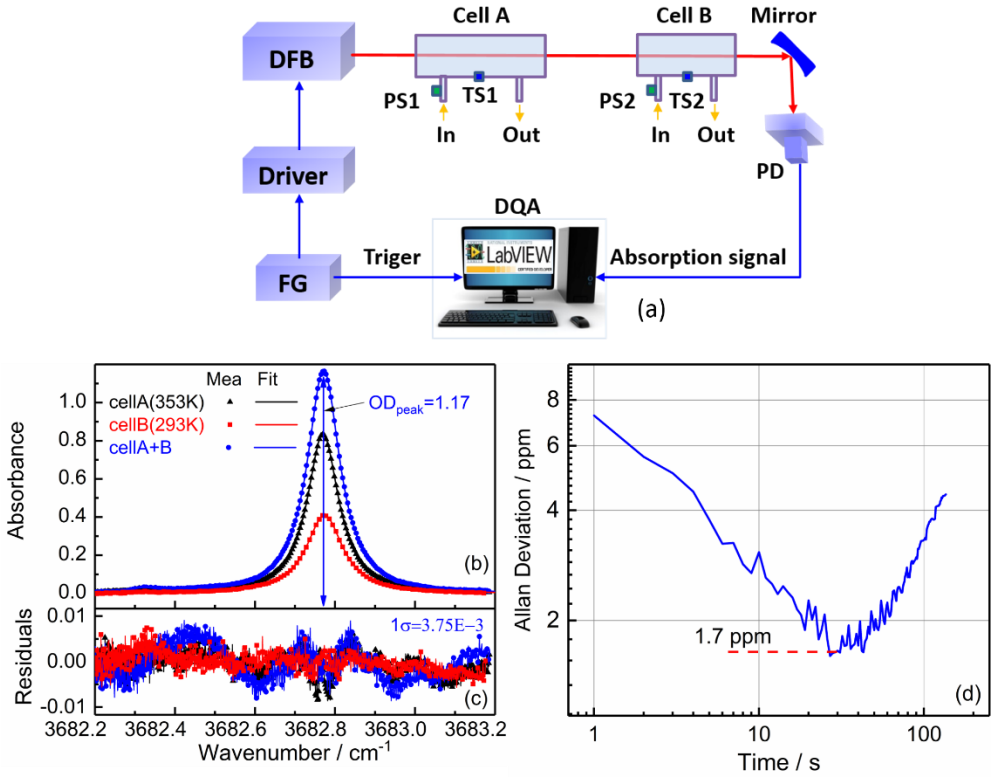

Figure 6. (a) Schematic drawing of the experimental TDLAS setup, PS-pressure sensor, TS-temperature sensor, PD-photodetector, FG-function generator, DQA-data acquisition card. (b) Measured CO_2 (P36e line, 770 mbar, 0.01 mol/mol CO_2 in N_2) spectra under different conditions; Triangle: cell A spectrum at 353 K; Square: cell B spectrum at 293 K; Circle: cell A+B spectrum under heterogeneous temperature condition. (c) The residuals of the Voigt fit to the measured data were shown in (b). (d) The Allan deviation plot of this spectrometer.

To generate the heterogeneous thermal boundary layers, two cells were used along the beam path with a total optical path length of 58 cm. Cell A with 38 cm path length can be heated up to 600°C by an electronic heating system (SITEC, 772.5011-K), while cell B was used at room temperature with 20 cm length. Pressure and temperature inside both cells WERE continuously measured by pressure sensors and PT100 temperature sensors.

The performance of the TDLAS spectrometer was evaluated in terms of sensitivity, precision and stability. The concentration of 0.01 mol/mol CO_2 in N_2 test gas was used in the experiments. The typical measured absorption profiles with fitted Voigt profiles are shown in Fig. 6b (averaged over 10 individual scans, Δt=3 s), as well as the residuals (Fig. 6c) between the measured data and the Voigt fitting. The 'Triangle' absorption spectrum was measured in the condition of heating cell A to 353 K (test gas pressure in cell A was 770 mbar) and evacuating cell B. The 'Square' spectrum was measured at cell B filled with test gas (T=293 K, p=770 mbar) while cell A was at vacuum. The measured spectrum under heterogeneous temperature condition is shown in 'Circle', the test gas temperatures in cell A and B were different, but the concentration and pressure were the same. These spectra and fitting residuals were used to

derive an estimate on the optical sensitivity of the spectrometer on short time scales of seconds. The residual can be quantified by the statistical standard deviation of the residual over the spectral range, 1σ equals the OD noise. The peak values on the optical density (OD = $-\ln(I/I_0)$) scale and the 1σ of residuals were compared as the signal-to-noise ratio (SNR). The SNR result is 312 for the circle curve in Fig. 6b. Dividing the concentration measured by the SNR, the noise equivalent concentration (NEC) or sensitivity is 32 ppm. It is also common to normalize the noise equivalent absorption coefficient with respect to the path length and the square root of the temporal bandwidth, which yields in this case 1.12×10^{-4} cm^{-1} $Hz^{-1/2}$. Note that all the spectra including those under heterogeneous conditions presented in this paper were fitted with Voigt profile. The Voigt fitting for the measured spectra worked well for all the experimental conditions, there was no significant increase in the residuals comparing to the fitting in homogeneous condition.

The precision and stability of the sensor were investigated by means of the Allan deviation as shown in Fig. 6d, which was recorded for a stable CO_2 concentration 0.01 mol/mol. The Allan deviation plot follows the general behavior, first the precision is improved with the integration time while white noise is reduced, then for the longer time periods the precision gets limited by the long-term instabilities like thermal drifts. At 1 s averaging time, a precision of 7.3 ppm can be achieved. The Allan deviation plot indicates that the precision can be further improved to 1.7 ppm at 30 s of integration time.

Deviation of concentration measurements

To investigate the concentration measurement with LOS TDLAS technique under heterogeneous temperature distribution conditions, cell A (T_2, L_2) was heated up to different temperatures from 293 to 430 K. In the experiments, only the temperature heterogeneity was introduced, while the pressure and CO_2 concentration in both cells were kept constantly the same. In this demonstration, the p_i and C_i (=C_{ave}) shown in Fig. 2b were the same for each subsection. The measured deviation Δx was calculated by comparing the measured concentration x and the input test gas concentration C_{ave}, which can be known by measuring under homogeneous condition or from the test gas supplier. Figure 7 shows the measured and simulated concentrations (a) and deviations (b) under different temperature heterogeneities. For all measurements, test gas temperature in cell B (T_1, L_1) was kept around room temperature (293 K), the pressure in both cells were 770 mbar. At each temperature point as shown by x-axis in Fig. 8 (test gas temperature in cell A), the path-integrated spectral area was fitted, then the concentration was obtained using Eqs. 2 and 5 with different calculation temperature (T_{ave}, T_{min} and T_{max}). The dots and dished line in Fig. 7 shows the measured results. The discrepancy between the derived concentrations with different calculation temperature increases as the temperature gradient increases. Also, the deviations increase as the temperature gradient increases for all curves. For clarity, only one error bar was shown for the first data point in Fig. 7a. The relative uncertainty of concentration measurement was about 2% (k=2), that's the reason why the measured results are scattered. With the simulation method discussed in section 2, the deviations (concentrations) were simulated for each condition with different calculation temperature as shown in Fig. 7 (solid lines). The measured concentrations from path-integrated spectra and deviations are in good agreement with the simulation results. This verifies the proposed simulation methodology in section 2.

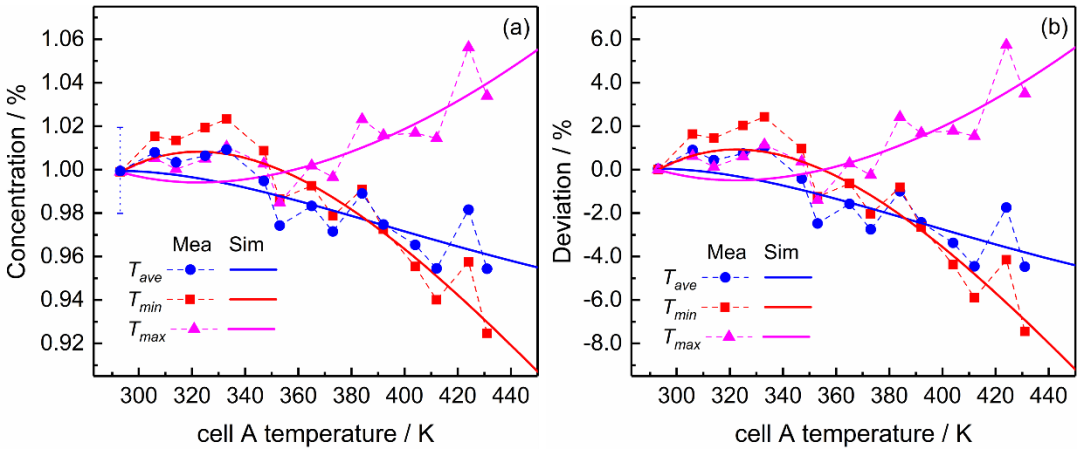

Figure 7. (a) Comparison of the measured and simulated concentration with different calculation temperatures. (b) The corresponding devotions.

Collisional width under heterogeneous conditions

By holding the Doppler width fixed at the calculated value during Voigt fitting for the path-integrated spectrum, the collisional width (full width half maximum, FWHM) is extracted from the overall width of the absorption profile. The temperature dependence is determined by performing a power function fit of the measured collisional widths at various temperatures as shown in Fig. 8a. Note that the first and second terms on the left side of Eq. 4 are combined, one temperature dependence, n_{all}, was fitted. The spectra analyzed here were same as those used in Fig. 7, and the Doppler widths were calculated based on the path-averaged temperature T_{ave}. The collisional widths were extracted from the spectra under both homogenous (Square) and heterogenous conditions (Circle). The measured widths under homogenous conditions show good agreement with exponential fit as described by Eq. 5 leading to a value of R^2 =0.993. The measured n_{all} is 0.77±0.02 for the CO_2 P36e line in N_2 gas matrix (HITRAN2012 database n_{air}=0.76). While, the measured n_{all} based on the collisional widths extracted from heterogenous conditions is incorrect. The larger the temperature gradient, the larger the discrepancy between the collisional widths of homogenous and heterogenous conditions is observed.

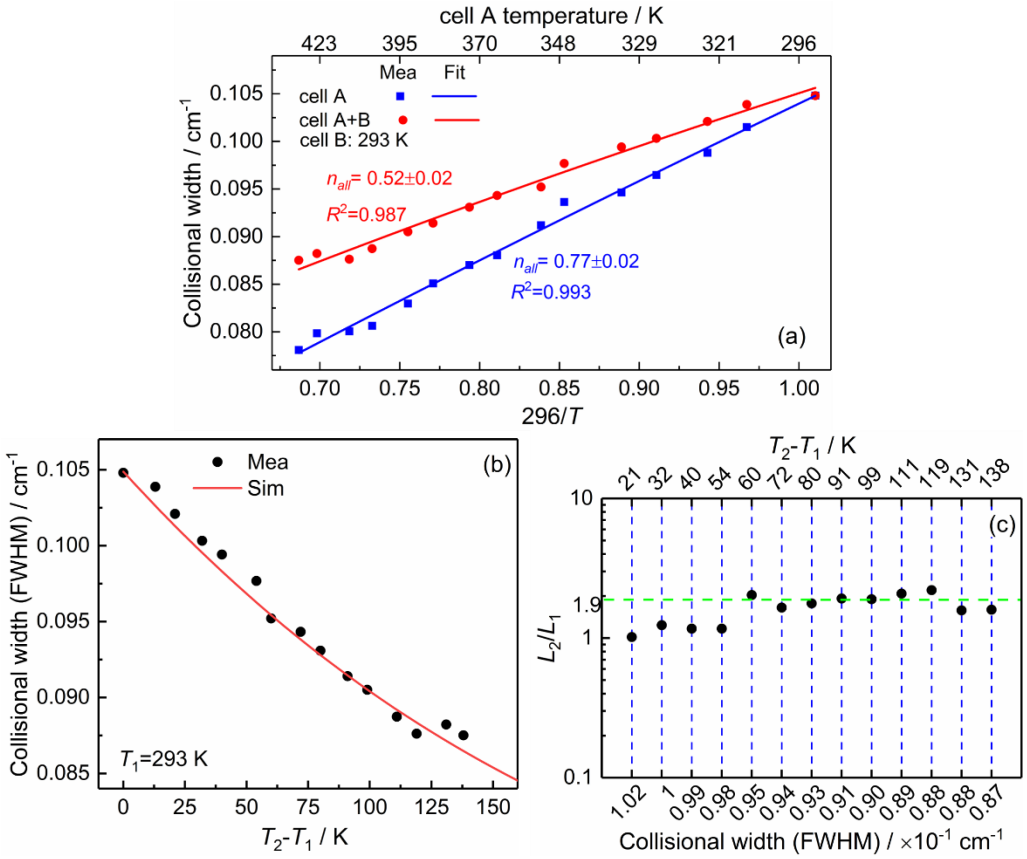

Figure 8. (a) Measured temperature dependence of the collisional width under homogeneous (Square) and heterogeneous (Circle) conditions, and the nonlinear fits. (b) Comparison of measured and simulated collisional width under heterogeneous conditions. (c) The calculated thermal boundary layer ratios using the measured collisional width based on Fig. 5b.

The measured collisional widths were compared with the simulated values from Fig. 5b, as shown in Fig. 8b. The measured results are in excellent agreement with the simulated collisional widths under the conditions with different thermal boundary layers. As discussed in section 2.5, the thermal boundary layer thickness can be estimated when knowing the collisional width, T_1 and T_2. First, the relation between the collisional width and the ratio of L_2/L_1 for certain T_1 and T_2 temperatures should be simulated as shown in Fig. 5a. Then, the L_2/L_1 ratio can be derived by addressing the measured collisional width value on the simulated relationship curve. The estimated L_2/L_1 ratios were shown in Fig. 8c for different heterogeneities, the green line indicates the real cell length ratio L_2/L_1 =1.9 in the experiment. For large temperature gradients, the estimated L_2/L_1 ratios are closer to the true value. While simulating the relation between the collisional width and the ratio of L_2/L_1, an initial gas concentration is needed. For the gas species with very low concentration (e.g. <1%), the first term on the left side of Eq. 4 is rather small comparing with the second term. The initial gas concentration in the simulation is not crucial for using the collisional width to estimate the thermal boundary layer information. But while the target gas has high concentration i.e. >10~20%, it is necessary to have the knowledge of the concentration when doing the simulation.

Conclusion

We have developed a new methodology for quantifying the thermal boundary layer effects on LOS TDLAS measurements. A dTDLAS spectrometer with two gas cells was implemented to achieve the temperature heterogeneities along the LOS and validate the simulation results. The spectrometer was applied to the detection of CO_2 concentrations and collisional widths under homogenous and heterogenous conditions using different calculation temperatures (T_{ave}, T_{min} or

T_{max}). Open-path TDLAS instruments, despite being widely used, have so far rarely been investigated for LOS heterogeneity effects on concentration measurements, although they may be small. To our knowledge, the quantification of the effects of thermal boundary layers on LOS TDLAS based concentration and collisional width measurements has been presented for the first time. The simulated deviations, collisional widths and estimated boundary layer thickness show very good agreement with the experimental results. This method will facilitate further investigation of the performance (e.g. systematic deviations) of commercial TDLAS instruments used in conditions with temperature heterogeneities. Additionally, this simulation method can also be used to evaluate whether the transition line is suitable for certain heterogenous conditions with allowable deviation. Further measurements and simulations will be performed to extend the method to concentration and/or pressure heterogeneities.

Conflict of Interest

The authors report there are no conflicts of interest.

Funding

This work was supported by the IMPRESS project within the European Metrology Research Programme (EMRP). The EMRP is jointly funded by the EMRP participating countries within EURAMET and the European Union.

Reference

1. V. Ebert, J. Wolfrum. ‘‘Absorption Spectroscopy’’. In: F. Mayinger, O. Feldmann, editors. Optical Measurements–Techniques and Applications, 2nd corr. edition. (Heat and Mass Transfer), Heidel- berg, München: Springer Verlag, 2001. 227-265.

2. J. A. Nwaboh, Z. Qu, O. Werhahn, V. Ebert. ‘‘Interband cascade laser-based optical transfer standard for atmospheric carbon monoxide measurements’’. Appl. Opt. 2017. 56(11): E84-E93.

3. Z. Qu, E. Steinvall, R. Ghorbani, F. M. Schmidt. ‘‘Tunable Diode Laser Atomic Absorption Spectroscopy for Detection of Potassium under Optically Thick Conditions’’. Anal. Chem. 2016. 88 (7): 3754-60.

4. C. S. Goldenstein, R. M. Spearrin, J. B. Jeffries, R. K. Hanson. ‘‘Infrared laser-absorption sensing for combustion gases’’. Prog. Energy Combust. Sci. 2017. 60: 132-176.

5. R. K. Hanson. ‘‘Applications of quantitative laser sensors to kinetics, propulsion and practical energy systems’’. Proc. Combust. Inst. 2011. 33(1): 1-40.

6. X. Ouyang, P. L. Varghese. ‘‘Line-of-sight absorption measurements of high temperature gases with thermal and concentration boundary layers’’. Appl. Opt. 1989. 28(18): 3979-3984.

7. S. Cięszczyk. ‘‘A Local Model and Calibration Set Ensemble Strategy for Open-Path FTIR Gas Measurement with Varying Temperature’’. Metrol. Meas. Syst. 2013. 20(3): 513-524.

8. Z. Qu, R. Ghorbani, D. Valiev, F. M. Schmidt. ‘‘Calibration-free scanned wavelength modulation spectroscopy--application to H_2O and temperature sensing in flames’’. Opt. Express 2015. 23 (12): 16492-16499.

9. S. Wagner, B. T. Fisher, J. W. Fleming, V. Ebert. ‘‘TDLAS-based in situ measurement of absolute acetylene concentrations in laminar 2D diffusion flames’’. Proc. Combust. Inst. 2009. 32 (1): 839-846.

10. J. Wang, M. Maiorov, J. B. Jeffries, D. Z. Garbuzov, J. C. Connolly, R. K. Hanson. ‘‘A potential remote sensor of CO in vehicle exhausts using 2.3 μm diode lasers’’. Meas. Sci. Technol. 2000. 11 (11): 1576.

11. A. Sepman, Y. Ögren, Z. Qu, H. Wiinikka, F. M., Schmidt. ‘‘Real-time in situ multi-parameter TDLAS sensing in the reactor core of an entrained-flow biomass gasifier’’. Proc. Combust. Inst. 2017. 36 (3): 4541-4548.

12. S. Wagner, M. Klein, T. Kathrotia, U. Riedel, T. Kissel, A. Dreizler, V. Ebert. ‘‘Absolute, spatially resolved, in situ CO profiles in atmospheric laminar counter-flow diffusion flames using 2.3 μm TDLAS’’. Appl. Phys. B: Lasers Opt. 2012. 109 (3): 533-540.

13. J. Girard, R. Spearrin, C. Goldenstein, R. K. Hanson. ‘‘Compact optical probe for flame temperature and carbon dioxide using interband cascade laser absorption near 4.2 μm’’. Combust. Flame 2017. 178: 158-167.

14. K. Sun, R. Sur,; X. Chao, J. B. Jeffries, R. K. Hanson, R. J. Pummill, K. J. Whitty. ‘‘TDL absorption sensors for gas temperature and concentrations in a high-pressure entrained-flow coal gasifier’’. Proc. Combust. Inst. 2013. 34 (2): 3593-3601.

15. C. S. Goldenstein, C. A. Almodóvar, J. B. Jeffries, R. K. Hanson, C. M. Brophy. ‘‘High-bandwidth scanned-wavelength-modulation spectroscopy sensors for temperature and H2O in a rotating detonation engine’’. Meas. Sci. Technol.2014. 25 (10): 105104.

16. C. S. Goldenstein, I. A. Schultz, J. B. Jeffries, R. K. Hanson. ‘‘Two-color absorption spectroscopy strategy for measuring the column density and path average temperature of the absorbing species in nonuniform gases’’. Appl. Opt. 2013. 52 (33): 7950-62.

17. F. Li, X.Yu, W. Cai, L. Ma. ‘‘Uncertainty in velocity measurement based on diode-laser absorption in nonuniform flows’’. Appl. Opt. 2012. 51 (20): 4788-4797.

18. L. S. Chang, C. L. Strand, Jeffries, J. B. Jeffries, R. K. Hanson. G. S. Diskin, R. L. Gaffney, D. P. Capriotti. ‘‘Supersonic Mass-Flux Measurements via Tunable Diode Laser Absorption and Nonuniform Flow Modeling’’. AIAA J. 2011. 49 (12): 2783-2791.

19. M. Schoenung, R. K. Hanson. ‘‘CO and Temperature Measurements in a Flat Flame by Laser Ab orption Spectroscopy and Probe Techniques’’. Combust. Sci. Technol.1980. 24 (5-6): 227-237.

20. W. Cai, C. F. Kaminski. ‘‘Tomographic absorption spectroscopy for the study of gas dynamics and reactive flows’’. Prog. Energy Combust. Sci. 2017. 59: 1-31.

21. X. Liu, J. B. Jeffries, R. K. Hanson. ‘‘Measurement of Non-Uniform Temperature Distributions Using Line-of-Sight Absorption Spectroscopy’’. AIAA J. 2007. 45 (2): 411-419.

22. S. T. Sanders, J.Wang, J. B. Jeffries, R. K. Hanson. ‘‘Diode-laser absorption sensor for line-of-sight gas temperature distributions’’. Appl. Opt. 2001. 40 (24): 4404-4415.

23. C. Liu; L. Xu, Z. Cao. ‘‘Measurement of nonuniform temperature and concentration distributions by combining line-of-sight tunable diode laser absorption spectroscopy with regularization methods’’. Appl. Opt. 2013. 52 (20): 4827-4842.

24. A. Seidel, S. Wagner, A. Dreizler, V. Ebert. ‘‘Robust, spatially scanning, open-path TDLAS hygrometer using retro-reflective foils for fast tomographic 2-D water vapor concentration field measurements’’. Atmos. Meas. Tech. 2015. 8 (5): 2061-2068.

25. A. Pogány, S. Wagner, O. Werhahn, V. Ebert. ‘‘Development and metrological characterization of a tunable diode laser absorption spectroscopy (TDLAS) spectrometer for simultaneous absolute measurement of carbon dioxide and water vapor’’. Appl. Spectrosc. 2015. 69 (2): 257-268.

26. N. Lüttschwager, A. Pogány, J. Nwaboh, A. Klein, B. Buchholz, O. Werhahn, V. Ebert. ‘‘In Traceable amount of substance fraction measurements in gases through infrared spectroscopy at PTB’’. 17th International Congress of Metrology 2015. EDP Sciences: 07005.

27. L.S. Rothman, I.E. Gordon, Y. Babikov, A. Barbe, D. Chris Benner, P.F. Bernath, M. Birk, L. Bizzocchi, V. Boudon, L.R. Brown, A. Campargue, K. Chance, E.A. Cohen, L.H. Coudert, V.M. Devi, B.J. Drouin, A. Fayt, J.-M. Flaud, R.R. Gamache, J.J. Harrison, J.-M. Hartmann, C. Hill, J.T. Hodges, D. Jacquemart, A. Jolly, J. Lamouroux, R.J. Roy Le, G. Li, D.A. Long, O.M. Lyulin, C.J. Mackie, S.T. Massie, S. Mikhailenko, H.S.P. Mu¨ller, O.V. Naumenko, A.V. Nikitin, J. Orphal, V. Perevalov, A. Perrin, E.R. Polovtseva, C. Richard, M.A.H. Smith, E. Starikova, K. Sung, S. Tashkun, J. Tennyson, G.C. Toon, V.G. Tyuterev, J. Vander Auwera, G. Wagner. ‘‘The HITRAN2012 Molecular Spectroscopic Database’’. J. Quant. Spectrosc. Radiat. Transfer 2013. 130: 4-50.

28. A. Pogány, O. Ott, O. Werhahn, V. Ebert. ‘‘Towards traceability in CO2 line strength measurements by TDLAS at 2.7μm’’. J. Quant. Spectrosc. Radiat. Transfer 2013. 130: 147-157.